IEEE Access
Multidisciplinary | Rapid Review | Open Access Journal

Received September 30, 2020, accepted October 1, 2020, date of publication October 12, 2020, date of current version October 26, 2020.

Digital Object Identifier 10.1109/ACCESS.2020.3030005

The Correlation and Balance of Material Properties for DC Cable Insulation at Design Field

MATTEWOS TEFFERI[1,2], (Member, IEEE), MOHAMADREZA ARAB BAFERANI[1,2], HIROAKI UEHARA[3], (Member, IEEE), AND YANG CAO[1,2], (Senior Member, IEEE)

[1]Electrical Insulation Research Center, Institute of Materials Science, University of Connecticut, Storrs, CT 06269, USA
[2]Electrical and Computer Engineering, University of Connecticut, Storrs, CT 06269, USA
[3]Department of Science and Engineering, Kanto Gakuin University, Yokohama 236-8501, Japan

Corresponding author: Yang Cao (yang.cao@uconn.edu)

ABSTRACT The innovation of materials with disruptive properties can be efficiently guided by improved physical understanding of material design principles. The design of a polymeric insulation depends on the desired requirements of the specific application, which, in the case of DC cable insulation, can be stated in terms of the following properties: controlled electrical conductivity, low space charge accumulation and high breakdown strength. Full characterization and detailed understanding of these properties as well as their correlation and balance may bring the ability to engineer needed dielectric properties for using as DC cable insulation. The aim of this paper is to identify the optimal DC insulation design space and to develop a formalism of the correlation between the conductivity and space charge, guided by a relatively simple model based on two physical parameters, activation energy (ξ) and mean trap separation (λ). With respect to implications for practical material design, the study demonstrates that a polymer material with activation energies in the range of 0.4 to 0.5 eV with relatively high trap density (N) ($N = \lambda^{-3}$, $\lambda = 1$ nm, $N = 1\text{E} + 27\ \text{m}^{-3}$) can be suitable for HVDC cable insulation.

INDEX TERMS Conductivity, material design, direct current (DC), crosslinked polyethylene (XLPE), space charge, cable insulation, thermal gradient.

I. INTRODUCTION

The U.S. Energy Information Administration's (EIA) latest International Energy Outlook 2020 projects a relatively sharp growth in renewables from currently19% to 38% by 2050. The main part of this increase in renewable energy is from the wind and solar resources, up from about 50% share now to an estimated share of 80% in 2050. Declining prices for new wind and solar projects support the growing renewables share of the generation mix [1]. High voltage direct current (HVDC) and Medium voltage direct current (MVDC) are emerging rapidly as critical enablers for integrating (offshore) wind and solar renewables [2]–[6]. HVDC overhead lines for onshore- and HVDC cables for offshore- wind integrations have been built in Europe and planned in the US [7] to efficiently take advantage of this tremendous energy resource potential. Multi-terminal HVDC grid with voltage source converters emerges as one of the technical solutions for pooling and transmitting offshore wind energy to load centers located far away onshore.

To ensure the high performance of a HVDC cable system, the main and important DC electrical attributes of polymeric insulations shall be properly addressed, which include space charge characteristics, DC breakdown strength and electrical conductivity. Among them, nonlinear conduction in the dielectric plays an essential role in determining these DC characteristics, e.g., the temperature gradient induced ''inversion'' of the field across the cable insulation. In this regard, a small temperature coefficient of conductivity is desirable, in order to limit the temperature-induced change in conductivity across the dielectric and to limit the increase in conductivity from ambient temperature to maximum operating temperature. However, nonlinear conduction and the temperature coefficient of conductivity are (anti) correlated. For instance, an increase of the temperature coefficient of electrical conductivity can lead to a space charge enhancement and DC breakdown strength reduction. At the same time, the conductivity must be sufficiently field-dependent

The associate editor coordinating the review of this manuscript and approving it for publication was Chandan Kumar.

to control the field across the dielectric in the presence of the expected temperature gradient at operating temperature and electric field. Therefore, uncovering the interplay of these electrical characteristics becomes critical for the development of new polymeric DC insulation. In this paper, we present the relations between the most important electrical characteristics based on two basic parameters, i.e., the activation energy (ξ) and the mean trap separation (λ) [8], [9], with the hope that such basic understanding of those physical parameters will bring in the ability to engineer desirable DC material and shed light on the understanding the physical basis of aging and other phenomena in dielectrics [10]. These improved understandings contribute ultimately towards developing tailored polymeric insulation materials with desirable performance for new DC cables in future energy efficient electric power grids.

II. THE CORRELATION OF KEY DESIGN PARAMETERS

A. PHENOMENOLOGICAL CONDUCTION MODEL

Conductivity represents the key electrical property to be considered in the design of DC insulation system. Unlike the dielectric constant, the key constitutive parameter that grades field distribution under AC, which is nearly independent of the electric field and temperature, the conductivity is strongly dependent on operating temperature, electric field and material compositions. While the temperature dependent part of the conductivity often follows an Arrhenius relationship, the electric field dependency of the conductivity is very complex and strongly affected by the space charge distribution and dynamics across the insulation [8], [9].

A detailed one-dimensional conduction formalism constitutes the essential fundamental physics [11], but with a major disadvantage of containing too many variables, most of which are poorly known and often determined via somewhat arbitrary curve-fitting of experimental data. For instance, in the hopping conductivity function as shown in Equation (1), the temperature coefficient (ξ) can be determined experimentally, whereas the coefficient of the electric field (B) is hard to find. Given ''n'' from the guarded needle measurements [12], A and B can be determined in a variety of ways, e.g. by fitting to the measured data for σ(E,T), which does not always provide a good basis to derive the physical parameters of conductivity vs. electric field as the conductivity data are not reliable especially when measured at low electric field and temperature. Therefore, it would be desirable to model the electric field coefficient in terms of the temperature coefficient so that two variables could be reduced to one single variable.

Such an approach is valid because the temperature coefficient (ξ) and field coefficient (B) part of the conductivity are anti-correlated. More specifically, decreased temperature coefficient is correlated with increased field coefficient for fundamental physical reasons. This anti-correlation is not explicit in the common formulas for temperature and field dependent conductivity, yet this anti-correlation is very important in optimizing and balancing dielectric properties [8], [9]. Thus, any optimization of the dielectric in this context must balance the temperature and field dependence to control the electric field distribution under conditions of large thermal gradients.

To solve for the two unknowns (A and B) in equation (1), at least two boundary conditions are needed. Low field conductivity $\sigma(E_0, T_0)$ could be used as one boundary condition. We use a second boundary condition which couples the temperature and field-dependence of the conductivity through the space charge limiting field (SCLF). The SCLF at room temperature and 300 kHz ($\sim$1 μs rise time) is approximated by the ratio of activation energy to mean trap separation (ξ/λ, i.e., the energy gained between traps is comparable to the trap depth) [8], [9].

Thus, the correlation between temperature and field coefficients through λ allows us to determine appropriate connection between the activation energy and field-dependent conductivity by varying the trap density (N) ($N = \lambda^{-3}$). Based on the aforementioned boundary conditions, i.e., (1) value for $\sigma(E_0, T_0)$ (we adopt $\sim 10^{-15}$ S/m at 10kV/mm and 293K) and (2) the conductivity at the SCLF ($\sigma(E_{SCLF}) = \varepsilon\omega$), which is determined by the dielectric time constant of applied frequency [6], the two unknowns (A and B) are solved. Therefore, given A, B, n, and the $\Delta T = 15°C$, we can compute for the field at the inner and outer radii of the insulation based on the analysis in [8], [9], [11].

In addition to DC conductivity, space charge represents the other critical parameter in DC insulation design. The presence of space charge can lead to destructive electric field enhancements and result in failure of the insulation under DC operation. Space charge is caused by ionization of impurities, spatially inhomogeneous conductivity and charge injection from the electrodes. To quantify the space charge quantity in the insulation bulk associated with conductivity gradient, a general approach starting from the Maxwell equations can be used. This approach is valid at the design field under the assumption of ohmic contacts, i.e., neglecting space-charge accumulation due to injection (e.g., Schottky mechanism) [13], [14]. Equation (2) presents the contribution of space charge due to the thermal and electrical gradients. The accumulation of space charge with the temperature gradient has a major effect on the electric field grading with a load.

B. DESIGN CONSTRAINTS

1) POWER DISSIPATION

The load current flowing and the resistive heating in the conductor of a cable induce a thermal gradient over the cable insulation. In addition to the load current, leakage current flowing through the insulation, if not properly designed, may create a considerable loss and contribution to the heat generation which might lead to thermal runaway.

As shown in Equation (3), the power density of the insulation is governed by the DC conduction. Any increase in conductivity enhances the power density which may lead to the thermal runaway. Therefore, this constraint places a limit on the conductivity at maximum operating temperature and

TABLE 1. Key design parameters and physical basis for correlation.

No.	Key Parameter	Equation	Properties to be correlated
1	Conductivity	$\sigma(E,T) = A\exp\left(\frac{-\xi q}{k_B T}\right)\frac{\sinh\left(B\mid E\mid^n\right)}{\mid E\mid^n}$	$\xi \to B$
2	Space charge	$\rho_{tg} = -\varepsilon_0\varepsilon_r E(r)\left[\frac{\xi}{k_B T^2}\Delta T + \frac{B\coth(B\sqrt{E})}{2\sqrt{E}}\Delta E\right]$	$\xi \to \rho_{tg}$
3	Power Density	$Q = \sigma E^2 \Leftrightarrow \quad Q = \frac{2\Delta T}{\left(r_0^2 - r_i^2\right)\rho\ln\left(\frac{2L}{r_0}\right)}$	$\xi \to Q$
4	FEF	$FEF = 1 + \frac{E_{sc}}{E_{ave}}$	$\xi \to FEF$
5	Time constant	$\tau = \frac{\varepsilon_0\varepsilon_r}{\sigma(E,T)}$	$\xi \to \tau$

Note that σ is the DC conductivity (S/m), E is the electric field (V/m), ξ is the activation energy (eV), q is the charge electron (C), k_B is the Boltzmann constant (J/K), T is the temperature (K), A, B, and n are polymer related constants, ρ_{tg} is the thermal gradient generated space charge (C/m^3), ε_r is the relative permittivity, ε_0 is the permittivity of vacuum, Q is the power loss density (W/m^3).

field, especially under Type Test and other pre-qualification conditions when the cable is exposed to voltages of 1.85 times the nominal operating voltage level. Hence, when developing material for DC insulation, the ambition is to keep the conductivity as low as possible. A sufficiently low conduction depends also on the heat transfer conditions of the cable as well as on the intended design electric field.

For DC cable insulation with a power density Q (W/m^3), the total power dissipated per unit length will be $Q\pi(r_0^2 - r_i^2)$, where r_0 and r_i are the inner and outer radii of the insulation. Under the steady-state condition, for a cable of diameter d buried in a soil of ρ thermal resistivity (K-m/W) at depth L below the surface, an engineering approximation for the temperature rise at the outer diameter of the dielectric can be expressed by equation (3) [15], [16].

We calculate the maximum allowable power density by referring to a 150kV HVDC power cable with crosslinked insulation of 10 mm inner radius and 19 mm outer radius, installed 2m deep in soil of thermal resistivity of 0.8 m-K/W. If we assume maximum temperature rise of 1°C at the outer radius of the insulation, we obtain Q ≈ 2.0 kW/m^3. Therefore, for the aforementioned cable, the average power density within the dielectric should be less than 2.0 kW/m^3 at 90 °C and 40 kV/mm.

2) FIELD ENHANCEMENT FACTOR (FEF)

As hinted above, the accumulation of space charge can be the main accelerated degradation process in DC insulation. The space charges influence the electric field distribution in the cable insulation and can lead to failure especially after *polarity reversal* [13], [15]. Therefore, polymer insulating materials have to be characterized with least amount of space charge that only leads to minimal electric field distortion at the operating electric field and load conditions.

To quantify the influence of space charge on electric field distortion, FEF from equation (4), which is the ratio of the Laplacian electric field on average uniform electric field, is used. It is clear that FEF=1 is the ideal condition with uniform electric field.

3) TIME CONSTANT

The dielectric time constant is given by the ratio of permittivity to conductivity as shown in Equation (5). The dielectric time constant is a key parameter for determining the relaxation time for the redistribution of space charges within the insulation after voltage polarity reversal.

The importance of this time constant is that for the HVDC systems with line-commutated converters (LCC systems), when the polarity of the voltage is reversed back, the transition time from one polarity to the other is required to be less than 2 minutes based on CIGRE TB 496 [20]. If the relaxation time is faster than this transition time (2 minutes), the space charge can follow the change of voltage and thus the electric field enhancement during the polarity reversal process is thus considered minimum.

III. BALANCED PROPERTIES PROFILE

To understand the relation between different parameters, including activation energy, electric field coefficient, FEF, power density and space charge, a schematic diagram is depicted in Figure 1. In this diagram, the activation energy [eV] is used as a variable for the x-axis and other parameters are calculated based on the activation energy and depicted with desired unit on the y-axis. This diagram is generated to give a schematic overview of important material characteristics on the same scale. From Figure 1, it can be seen that

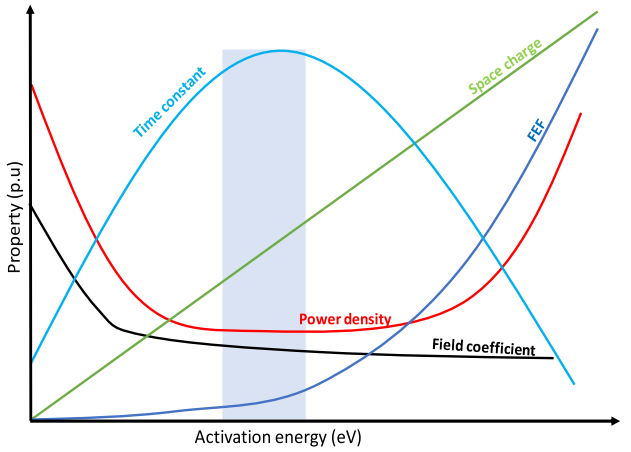

FIGURE 1. The balancing of Field coefficient, Power density, FEF, Space charge and Time constant of the material schematically drawn at maximum operating conditions as a function of the activation energy. In the shaded blue region, the properties are balanced to keep the power density and FEF minimum [8].

with increasing activation energy or temperature coefficient of conductivity, the electric field coefficient of conductivity decreases. In other words, although the reduction of activation energy leads to reduced dependency of electrical conductivity on temperature, it enhances the electrical conductivity dependency on the electric field (i.e., anti-correlated). Therefore, to have an optimal polymeric DC insulation, the dependency of electrical conductivity to temperature and electric field must be controlled at the normal operating electric field and maximum operating temperature. After the electric field coefficient (black curve) and temperature coefficient (x-axis) are correlated, the conductivity function is calculated. Then, the power dissipation (Q) at maximum operating electric field and temperature can be computed. As shown in the diagram, with the increase of the activation energy, power density of dielectric insulation firstly decreases and then increases.

In Figure 1, the dielectric time constant is in linear inverse relation with the conductivity, so at the peak of dielectric constant the conductivity is at minimum (the permittivity is constant). From this, a range of activation energies, the blue area in Figure 1, can be considered where the power density and FEF are low and safe from the thermal runaway. As the activation energy increases, it has a major effect on the field grading with load and results in an enhanced electric field distortion across the cable insulation which causes high FEF. Therefore, a desired dielectric material should be developed with optimum design parameters to ensure proper performance with right balance, as in the blue area [9], [18].

In summary, to engineer the desired electrical properties for cable insulation, two basic parameters, i.e. the activation energy (ξ) and the mean trap separation (λ) are critical to determining the electrical characteristics of dielectric. To understand the significance of these two parameters, two cases are studied. The only difference of these two cases are the different mean trap separation, and in each case the activation energy is varied from 0.2 eV to 1.0 eV and other parameters are calculated accordingly.

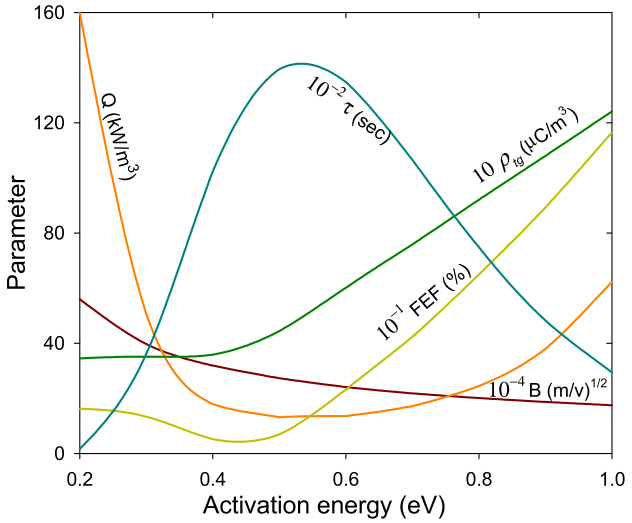

FIGURE 2. Calculated parameters at 30 kV/mm and 90°C for Case 1. The parameters are calculated by varying the activation energy from 0.2eV to 1eV with $\lambda = 3.0$ nm [8].

Case 1 (With λ=3.0 nm or Low Trap Density): In this case as it can be seen in Figure 2, FEF is acceptable; however, with the changing of the activation energy, the power density can reach a high value of more than 10 kW/m^3, indicating high probability of thermal runaway and failure of insulation.

Case 2 (With λ=1.0 nm or High Trap Density): If we reduce λ to 1 nm, the above situation (Figure 2) is improved significantly as seen in Figure 3. For ξ in the range of 0.2 eV to 0.9 eV, the power dissipation is less than 4 kW/m^3, which is manageable. In addition, the calculated time constant is less than 120 s which suggests proper design space for polarity reversal condition. It is worth noting that, for $\xi > 0.6$ eV, FEF can be significant.

Therefore, increasing the trap density (i.e., the mean separation between traps from $\lambda = 3$ nm to $\lambda = 1$ nm) leads to the reduction of power density and appropriate conduction characteristics for DC cable insulation.

IV. EXPERIMENTAL INVESTIGATION

A. SAMPLE PREPARATION

In this work, two kinds of polyethylene (PE) compounds were studied. One is the crosslinked PE (XLPE) used in HVDC cable and the other is XLPE used in HVAC cable. The samples were prepared from commercial pellets by press molding. Before the measurements, plaque samples were degassed for five days at 80 °C in a vacuum oven and kept in dry and clean laboratory conditions.

B. DC CONDUCTIVITY

The DC conductivity of plate samples were measured using a sample holder which was built based on ASTM 257 specifications. Samples of 250 μm in thickness were put in guarded stainless-steel electrodes for DC conductivity testing. The sample temperature was raised by heating the entire sample holder with a Delta Design 9023 environmental chamber.

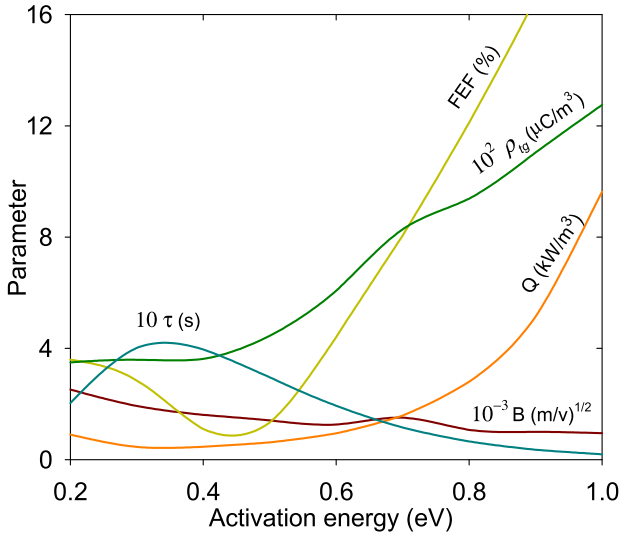

FIGURE 3. Calculated parameters at 30 kV/mm and 90°C for Case 2. The parameters are calculated by varying the activation energy from 0.2 eV to 1 eV with $\lambda = 1.0$ nm [8].

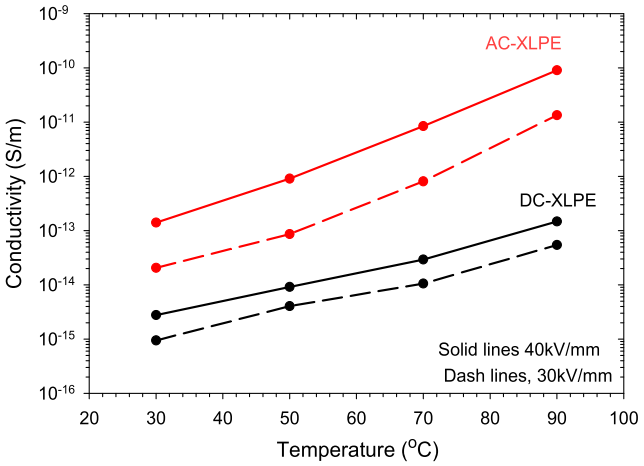

FIGURE 4. Measured DC conductivity as a function of temperature and electric field for AC-XLPE and DC-XLPE.

The steady-state conduction current was measured by using a Keithley 6514 electrometer for 5000 s. Since the measured current changes with time, an average quasi steady state value from 4500-5000 s of the measurement is used to obtain the conductivity value.

C. SPACE CHARGE

The space charge within the samples under dc voltage were measured using a pulse electroacoustics (PEA) technique. The space charge was calculated with the standard procedure [19]. The sound pressure at the piezoelectric sensor may be expressed as follows:

$$p(t) = \int_{-\infty}^{\infty} E\left(t - \frac{l}{v_e} - \frac{l}{v_p}\right)\rho(x)dx \tag{6}$$

where p(t) is the sound pressure at the sensor, E is the pulsed electric field, v_e is the sound velocity in the aluminum, v_p is the sound velocity in the polymer and ρ(x) is the charge density. For calibration, a sample with known space charge distribution was used. The signal was calibrated and measured as follows.

$$F[V(t)] = F[Q(v_p t)]F[E(t)]K(t) \tag{7}$$

where F[V(t)] is the sample/calibration signal, F[Q($v_p t$)] is the space-charge distribution, F[E(t)]K(v) is the fixed system related response.

The charge distribution in the samples was determined by:

$$Q(v_p t) = F^{-1}\left[F[Q_0(t)]\frac{F[V(t)]}{F[V_0(t)]}\right] \tag{8}$$

The acoustic pulse was excited in charge carrying sample by applying 350V pulse train with ~1 ns rise time at a repetition of 150 Hz. The acoustic waves were detected by a polyvinylidene fluoride (PVDF) piezoelectric sensor with a thickness of 9 μm. The output of PEA sensor was amplified for recording using a Tektronix DPO5034 oscilloscope with a sampling rate of 2.5 GS/s. All data traces were averaged over 5000 measurements before further digital signal processing.

To generate the thermal gradient across the thickness of the flat samples for simulating the ''loaded'' cable, an emulated thermal gradient was generated using thin-film heaters with resistance temperature detectors (RTD) applied to the top and bottom surface of the PEA test cell and close to the samples as feedback controls. This was achieved with a heating power of 20W and with the whole system placed into an oven at 50°C. Details of the experimental setup have been presented in our previous publication [21]–[23].

V. RESULT AND ANALYSIS

A. DC CONDUCTIVITY

The DC conductivity was obtained from the quasi steady-state current measurement at different temperatures from 30 °C to 90 °C. Figure 4 shows the DC conductivity at 30 kV/mm and 40 kV/mm. The value of the activation energy for the conduction process can be obtained from the Arrhenius relationship of $log\ \sigma$ vs. T^{-1} at a given field as a function of temperature, as shown by equation (9).

$$\sigma(E, T) = \sigma_0 \exp\left(\frac{-\xi q}{k_B T}\right) \tag{9}$$

The measured activation energies (ξ) and conductivity at reference temperature (σ_0) are summarized in Table. 2.

TABLE 2. Conductivity parameters of equation (9) for AC-XLPE and DC-XLPE.

Material	σ_0 (S/m)	(ξ) (eV)
AC-XLPE	1.1E+3	1.0
DC-XLPE	1.8E-5	0.6

The AC-XLPE material has higher activation energy compared to DC-XLPE. The implication of activation energy for HVDC cable insulation is demonstrated by solving the

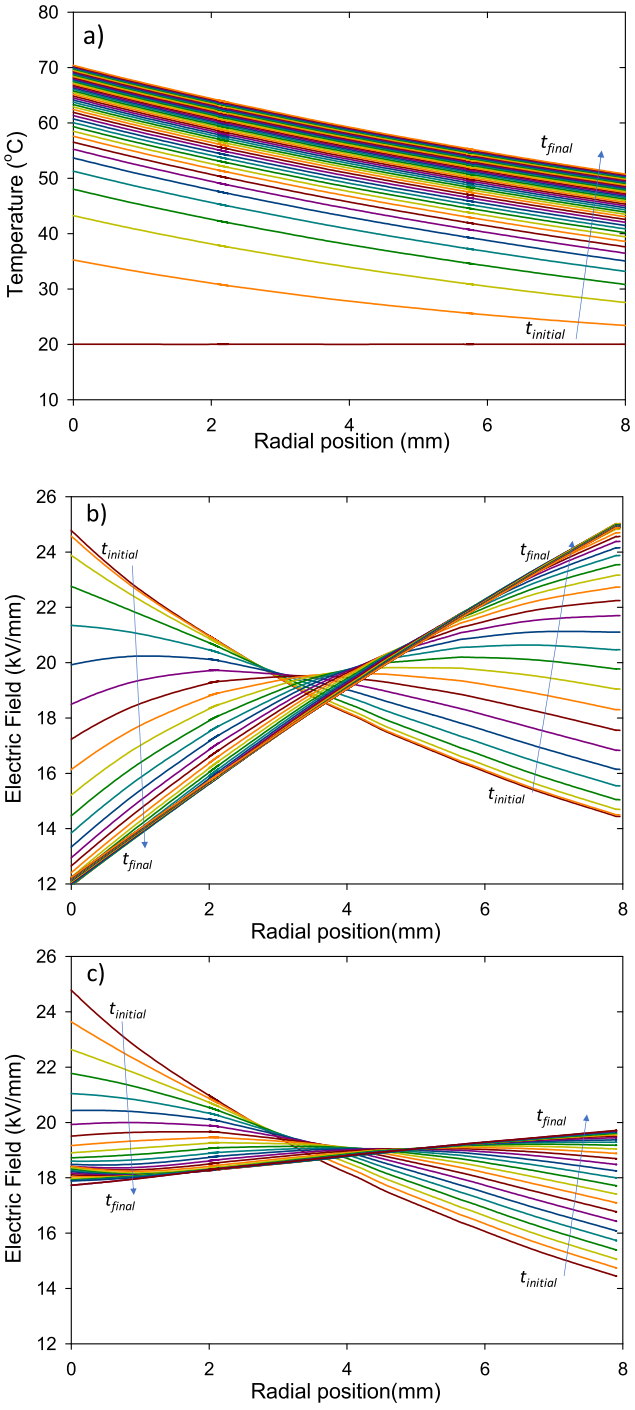

FIGURE 5. a) Temporal and spatial distribution of temperature across the cable insulation. The thermal gradient is ∼ 15°C. b) Electric field grading for AC-XLPE and c) DC-XLPE. The field distribution is initially Laplacian and evolves gradually to resistive field distribution under full load conditions as shown by the arrow.

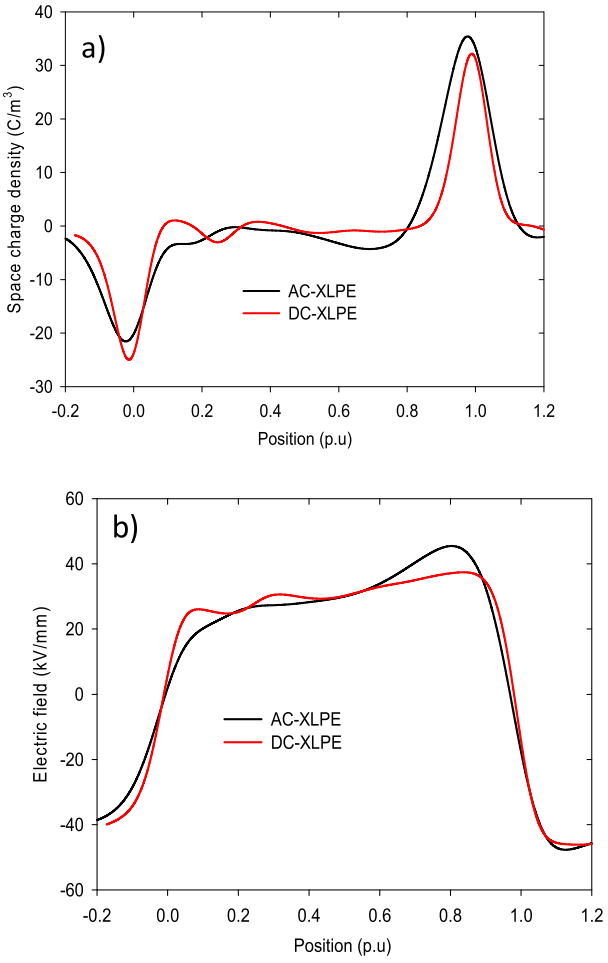

FIGURE 6. The space charge distributions (a) and Electric field distribution (b) of AC-XLPE and DC-XLPE at 30 kV/mm.

electric field distribution with a transient nonlinear computational tool for a cable with dimensions presented in Section II. Figure 5a shows the temperature distribution across the insulation. In this figure, the conductor is at 70 °C while the ground shield is at 55°C ($\Delta T = 15°C$). As illustrated in Figure 5b for the case of AC-XLPE, the field strength on the inner conductor is higher than inner conductor (c.a., "*field inversion*"). In contrast, for the case of DC-XLPE with lower activation energy of 0.6 eV, the field grading across the cable insulation is nearly uniform, as shown in Figure 5c.

In addition to the electric field distribution, the conductivity of AC-XLPE at 40 kV/mm and 90 °C is about 10^{-10} S/m which results in a power density of about 160 kW/m^3, which is considered high. For the case of DC-XLPE, the conductivity is about 2×10^{-13} S/m which results in a proper power density of about 320 W/m^3. Thus, the critical challenges are related to deep traps which are the possible cause for space charge accumulation as well as for high electrical conductivity at rated electric field and temperature. Therefore, reducing the trap depth (ξ) produces conduction characteristics suitable for HVDC cable dielectric.

B. SPACE CHARGE DISTRIBUTION CHARACTERISTICS

Figure 6 shows the space charge profiles of AC-XLPE and DC-XLPE at 30 kV/mm under 50 °C and a thermal gradient of 1 °C/mm measured by PEA. The accumulated heterocharges near the anode cause the electric field enhancement at the interface. The space charge in AC-XLPE tends to build

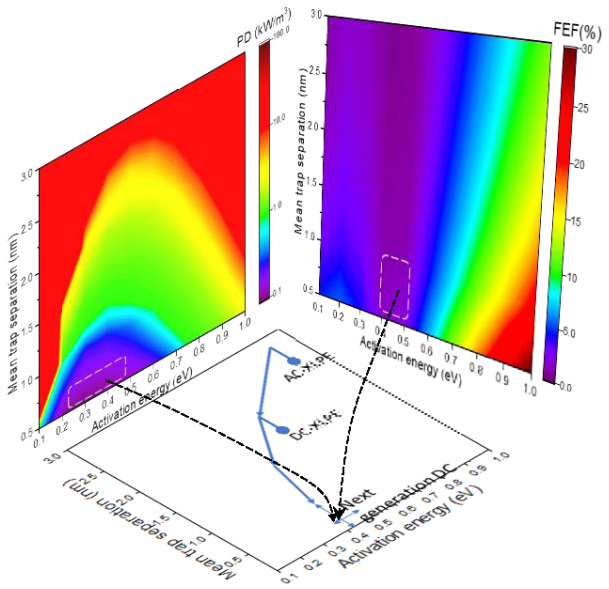

FIGURE 7. A Cartography of the two design constraints PD and FEF calculated as function of activation energy and mean trap separation. The AC-XLPE shows a higher PD and FEF. For the case of DC-XLPE the risk of thermal runaway is very small and FEF is improved. The future optimal DC insulation can be achieved with activation energy in the range of 0.4-0.5 eV with relatively high trap density (λ<1nm) [8].

up close to the anode resulting in a maximum field reaching 45 kV/mm (FEF=50%). Compared to the AC-XLPE, the accumulated space charge is less for the DC-XLPE, with the maximum field reaching about ∼37 kV/mm (FEF=23%).

Figure 7 shows the summary of the study for the optimal design space of polymeric DC insulation. In Figure 7, by varying the activation energy (ξ) and mean trap separation (λ), two main parameters which limit the design space, PD and EFE were calculated and depicted in color map. As it can be seen, in the range of $0.25 < \xi < 0.5$ eV and $\lambda < 0.5$ nm, PD is considered suitable. Moreover, the future optimal design space for the next generation of HVDC/MVDC cable system appears in the range of for the activation energy with the relatively high trap density ($\lambda < 1$ nm).

VI. CONCLUSION

DC cable possesses many design challenges mainly related to the temperature and field dependent properties of the insulation material. Hence, DC cable dielectrics require optimization to design for the desired properties. This paper introduces a phenomenological conduction formalism, based on which the conduction in DC cable insulation is analyzed to correlate key DC parameters as well as for their implications on material design. This simple model approach is based on two physical parameters, activation energy (ξ) and mean trap separation (λ), yet allows effective correlation to practical design to derive predicted properties and to validate against the experimental data, with the following major findings:

i. Following the design principles, the DC conductivity and space charge were characterized on two different grades of XLPE. The activation energy of AC-XLPE is found to be 1eV while for DC-XLPE is about 0.6 eV. The conductivity of AC-XLPE is two orders of magnitude higher than DC-XLPE. This may result in excessive power dissipation) density and hence thermal runaway. Also, from PEA measurement, the FEF of AC-XLPE is found higher than DC-XLPE.
ii. Using a transient nonlinear computational tool, the time dependent electric field distribution is evaluated for a model cable to provide insight into the reliability of DC power cables. The significance of low thermal activation energy of conductivity in controlling the DC electric field distribution under load condition is highlighted.
iii. A refined material design space is further presented. The study suggests an optimal DC insulation can be designed with an activation energy in the range of 0.4 - 0.5 eV with relatively high trap density ($\lambda \sim 1$ nm).

ACKNOWLEDGMENT

The authors would like to thank Prof. S. Boggs for many discussions during the beginning of this study.

REFERENCES

[1] *International Energy Outlook 2020 With Projections to 2050*, U.S. Energy Inf. Admin. (EIA), Washington, DC, USA, Jan. 2020.
[2] G. C. Montanari and P. Seri, "HVDC and UHVDC polymeric cables: Feasibility and material development," *IEEE Elect. Insul. Mag.*, vol. 35, no. 5, pp. 28–35, Sep. 2019.
[3] C. W. Gellings, "A globe spanning super grid," *IEEE Spectr.*, vol. 52, no. 8, pp. 48–54, Aug. 2015.
[4] P. Deane and M. Brinkerink, "Connecting the continents—A global power grid," *IEEE Power Energy Mag.*, vol. 18, no. 2, pp. 121–127, Mar. 2020.
[5] G. Chen, M. Hao, Z. Xu, A. Vaughan, J. Cao, and H. Wang, "Review of high voltage direct current cables," *CSEE J. Power Energy Syst.*, vol. 1, no. 2, pp. 9–21, 2015.
[6] Y. Zhou, S. Peng, J. Hu, and J. He, "Polymeric insulation materials for HVDC cables: Development, challenges and future perspective," *IEEE Trans. Dielectr. Electr. Insul.*, vol. 24, no. 3, pp. 1308–1318, Jun. 2017.
[7] J. Kumagai, "The U.S. Finally goes big on offshore wind," *IEEE Spectr.*, vol. 56, no. 1, pp. 25–26, Jan. 2019.
[8] M. Tefferi, S. A. Boggs, and Y. Cao, "The 'materials space' of DC polymeric dielectrics," in *Proc. IEEE Electr. Insul. Conf. (EIC)*, Jun. 2017, pp. 429–432.
[9] M. Tefferi, Z. Li, H. Uehara, and Y. Cao, "The correlation and balance of critical material properties for DC cable dielectrics," in *Proc. IEEE Conf. Electr. Insul. Dielectr. Phenomena (CEIDP)*, Oct. 2018, pp. 46–49.
[10] Z. Li, B. Du, C. Han, and H. Xu, "Trap modulated charge carrier transport in polyethylene/graphene nanocomposites," *Sci. Rep.*, vol. 7, no. 1, p. 4015, Dec. 2017.
[11] S. Boggs, D. H. Damon, J. Hjerrild, J. T. Holboll, and M. Henriksen, "Effect of insulation properties on the field grading of solid dielectric DC cable," *IEEE Trans. Power Del.*, vol. 16, no. 4, pp. 456–461, Oct. 2001.
[12] S. Boggs, "Very high field phenomena in dielectrics," *IEEE Trans. Dielectr. Electr. Insul.*, vol. 12, no. 5, pp. 929–938, Oct. 2005.
[13] D. Fabiani, G. C. Montanari, C. Laurent, G. Teyssedre, P. H. F. Morshuis, R. Bodega, and L. A. Dissado, "HVDC cable design and space charge accumulation—Part 3: Effect of temperature gradient," *IEEE Electr. Insul. Mag.*, vol. 24, no. 2, pp. 5–14, Mar. 2008.
[14] G. Montanari, "Bringing an insulation to failure: The role of space charge," *IEEE Trans. Dielectr. Electr. Insul.*, vol. 18, no. 2, pp. 339–364, Apr. 2011.
[15] J. H. Neher, "The temperature rise of buried cables and pipes," *Trans. Amer. Inst. Electr. Eng.*, vol. 68, no. 1, pp. 9–21, Jul. 1949, doi: 10.1109/T-AIEE.1949.5059897.

[16] C. A. Bauer and R. J. Nease, "A study of the superposition of heat fields and the kennelly formula as applied to underground cable systems," *Trans. Amer. Inst. Electr. Eng., III, Power App. Syst.*, vol. 76, no. 3, pp. 1330–1333, Apr. 1957, doi: 10.1109/AIEEPAS.1957.4499787.
[17] T. L. Hanley, R. P. Burford, R. J. Fleming, and K. W. Barber, "A general review of polymeric insulation for use in HVDC cables," *IEEE Elect. Insul. Mag.*, vol. 19, no. 1, pp. 13–24, Jan. 2003.
[18] M. Tefferi, L. Chen, S. Nasreen, H. Uehara, R. Ramprasad, and Y. Cao, "Tailoring polymeric insulation materials for DC cable dielectrics," in *Proc. IEEE Conf. Electr. Insul. Dielectr. Phenomena (CEIDP)*, Oct. 2019, pp. 773–776.
[19] O. Gallot-Lavallée, V. Griseri, G. Teyssedre, and C. Laurent, "The pulsed electro-acoustic technique in research on dielectrics for electrical engineering. Today's achievements and perspectives for the future," 2006, Art. no. ffhal-00019788.
[20] *Recommendations for testing DC extruded cable systems for power transmission at a rated voltage up to 500 kV*, CIGRE TBParis, France, 2012, vol. 496.
[21] M. Tefferi, Z. Li, H. Uehara, Q. Chen, and Y. Cao, "Characterization of space charge and DC field distribution in XLPE and EPR during voltage polarity reversal with thermal gradient," in *Proc. IEEE Conf. Electr. Insul. Dielectr. Phenomenon (CEIDP)*, Oct. 2017, pp. 617–620.
[22] H. Uehara, Z. Li, Q. Chen, G. C. Montanari, and Y. Cao, "Space charge behavior under thermal gradient in cross-linked polyethylene and ethylene-propylene rubber," *Sens. Mater.*, vol. 29, pp. 1199–1212, 2017.
[23] M. Tefferi, Z. Li, Y. Cao, H. Uehara, and Q. Chen, "Novel EPR-insulated DC cables for future multi-terminal MVDC integration," *IEEE Elect. Insul. Mag.*, vol. 35, no. 5, pp. 20–27, Sep. 2019.

MATTEWOS TEFFERI (Member, IEEE) received the M.Sc. degree in electric power engineering from the Chalmers University of Technology, Sweden, in 2013, and the Ph.D. degree in electrical engineering from the University of Connecticut, in 2019, working in the area of dielectrics. He is currently with the G&W Electric, Bolingbrook, IL.

MOHAMADREZA ARAB BAFERANI received the B.Sc. degree in electrical engineering from the Iran University of Science and Technology, Iran, and the M.Sc. degree from the University of Tehran, Iran. He is currently pursuing the Ph.D. degree in electrical engineering with the University of Connecticut. He is also a Graduate Research Assistant with the University of Connecticut. His main research interests are high voltage engineering, HVDC cable systems, composite polymeric insulations, and fault current limiters.

HIROAKI UEHARA (Member, IEEE) received the B.E., M.E., and Ph.D. degrees from Meiji University, Japan, in 1995, 1997, and 2000, respectively. In 2000, he joined the staff of the College of Engineering, Kanto Gakuin University, Japan. He was a Visiting Research Scholar with the University of Connecticut, from April 2014 to March 2015. Since 2013, he has been a Professor with Kanto Gakuin University. His research interests are in insulating materials, dielectrics, and electrostatic transducers.

YANG CAO (Senior Member, IEEE) received the B.S. and M.S. degrees in physics from Tongji University, Shanghai, China, and the Ph.D. degree from the University of Connecticut, in 2002. He served as a Senior Electrical Engineer with the GE Global Research Center, until 2013. He is currently a Full Professor with the Electrical and Computer Engineering Department, University of Connecticut. He is also the Director of the Electrical Insulation Research Center, Institute of Materials Science and the Site Director of the NSF iUCRC Center on High Voltage/Temperature Materials and Structures. His research interests are in the physics of materials under extremely high field and the development of new dielectric materials, particularly the polymeric nanostructured materials, for energy efficient power conversion and renewables integrations, as well as for novel medical diagnostic imaging devices.